Pan-cancer survey and evaluation of the oncogenic role of NF-κB1

Lihong Huang
Affiliated Hospital of Guilin Medical University
ruoling zheng
Guilin Medical University
Huasong Gong (gonghs556@163.com)
Yongchao Qiao (qiaoyc@glmc.edu.cn)

Research Article

Keywords: NF-κB1, cancer, survival analysis, bioinformatic analysis, immune

Posted Date: December 20th, 2021

DOI: https://doi.org/10.21203/rs.3.rs-1181290/v1

Abstract

Although emerging cells or animals based evidence supports an association between nuclear factor kappa-B1 (NF-κB1) cells and cancers, there has no pan-cancer analysis. Therefore, based on TCGA (The Cancer Genome Atlas) and GEO (Gene Expression Omnibus) data sets, we first studied the potential carcinogenic effect of NF-κB1 in 33 tumors. As we not only found high expression of NF-κB1 in most tumors, but also found that NF-κB1 expression is closely related to the prognosis of tumor patients. Enhanced phosphorylation of S893 was observed in several tumors, such as breast cancer, uterine corpus endometrial carcinoma or lung adenocarcinoma. In thymoma, NF-κB1 expression was relevant to $CD8^+$ T-cell infiltration levels, and tumor-associated fibroblast infiltration has also seen in other tumors, such as uterine corpus endometrial carcinoma or glioblastoma multiforme. In addition, the functional mechanism of NF-κB1 also involves the related functions of protein processing and RNA metabolism. In this study, NF-κB1 was pan-cancer study in order to have a systematic and comprehensive understanding of the carcinogenic effect of NF-κB1 in different tumors.

1 Introduction

The inhomogeneity of tumorigenesis. It is very important to analyze the pan cancer expression of any gene of interest to evaluate its relevance to clinical prognosis and potential molecular mechanism. We were able to conduct pan cancer analysis because the government funded TCGA project and the existing geo database contain functional genomics data sets of different tumors (1–3).

NF-κB1 (nuclear factor kappa B subunit 1) is a protein complex that controls transcription of DNA, cytokine production, and cell survival. The current evidence strongly suggests that the abnormal activation of NF-κB1 signaling pathway is related to tumorigenesis. A great deal of key cellular processes are controlled by effectors of this pathway, including immune response and apoptosis, both sides of which are critical in the development of cancer (4). Structural/functional analysis of NF-κB1 has been studied in physiology and clinicopathology in different diseases (5–7). NF-κB1 gene consists of 24 exons, located on chromosome 4q24 (8). NF-κB1 encodes a 105kD protein, which could be co-translated by 26S proteasome to produce a 50kD protein (9). The multifunctional NF-κB1 protein has been studied in this research group, and the functional relationship between NF-κB1 protein and liver cancer (10) breast cancer (11, 12),, and ovarian cancer (13). However, based on large clinical data, there is currently no evidence of a pan-cancer association between NF-κB1 and various tumor types.

Our study used TCGA project and geo database for pan-cancer analysis of NF-κB1 for the first time. At the same time, the possible molecular mechanism of NF-κB1 in the pathogenesis or clinical prognosis of different tumors was discussed through factors such as gene expression, survival status, DNA methylation, genetic changes, protein phosphorylation, immune infiltration and related cellular pathways

2 Materials And Methods

2.1 Gene expression analysis

We are on timer2 (tumor immune estimation resource, version 2) website (http://timer.cistrome.org) Gene of_ Enter NF-κB1 in the de module. To observe the expression difference of NF-κB1 in specific tumors or different tumor subtypes of TCGA project, adjacent normal tissues and tumors. For certain tumors with highly limited or without normal tissues, such as TCGA-DLBC (Lymphoid Neoplasm Diffuse Large B-cell Lymphoma), TCGA-TGCT (Testicular Germ Cell Tumors), etc. We used the GEPIA2 (Gene Expression Profiling Interactive Analysis, version 2) “Expression Analysis-Box Plots” module web server (http://gepia2.cancer-pku,cn/#analysis) (14). If the *P*-value cutoff=0.01, $\log_2$ FC (fold change) cutoff=1, “Match TCGA normal and GTEx data”, the difference in expression between these tumor tissues and corresponding normal tissues in the GTEx (Genotype-Tissue Expression) database was obtained by box plots. In addition, through the "pathological stage map" module of depia2, we obtained the fiddle map of NF-κB1 expression in different pathological stages (stages I, II, III and IV) of all TCGA tumors. The expression data of the log2 [TPM (Transcripts per million) +1] transformation is used for the box or fiddle diagram.

The UALCAN portal website (http://ualcan.path.uab.edu/analysis-prot.html) is an analysis of cancer omics data interactive web resources, and it allows us to CPTAC (Clinical proteomic tumor analysis consortium) data sets to analyze protein expression (15). Here, we investigated the expression level of total protein or phosphorylated protein (phosphorylated at sites S851, S892, S893, S903, S907, T939, S944) of NF-κB1 (NP_001158884.1) between normal tissue and primary tumor by inputting “NF-κB1”. The existing data sets of CHOL (cholangiocarcinoma), DLBC (Lymphoid Neoplasm Diffuse Large B-cell Lymphoma), GMB (Glioblastoma multiforme), LAML (Acute Myeloid Leukemia), PAAD (Pancreatic adenocarcinoma), THYM (Thymoma) were selected.

2.2 Survival prognosis analysis

We used the survival map module of GEPIA2 (16) to obtain the OS (overall survival) and DFS (disease free survival) significance map data of NF-κB1 in all TCGA tumors. Cutoff-high (50%) and cutoff-low (50%) values were used as expression thresholds to split the high-expression and low-expression cohorts. The hypothesis test adopts log rank test, and the survival map is also from GEPIA2 survival analysis module.

2.3 Genetic alteration analysis

Login cBioPortal website (https://www.cbioportal.org/) (17, 18), in the quick select section, select TCGA pan cancer atlas studies, enter NF-κB1, and query the genetic variation characteristics of NF-κB1. In the cancer type summary module, the change frequency, mutation type and can (copy number change) results of all TCGA tumors can be observed. The NF-κB1 mutation site information can be displayed in the protein structure diagram or three-dimensional (3D) structure through the mutation module.

2.4 Immune infiltration analysis

We used the immune gene module of TIMER2 web server to explore the relationship between NF-κB1 expression and immune infiltration of all TCGA tumors, and selected immune cells of tumor associated fibroblasts and CD8 + T cells. The TIMER, CIBERSORT, CIBERSORT-ABS, QUANTISEQ, XCELL, MCPCOUNTER and EPIC apply algorithms to estimate immune penetration. *P*-value and partial derivative correlation (COR) value were adjusted by purity Spearman rank correlation. The data are visualized as heat maps and scatter diagrams.

2.5 NF-κB1-related gene enrichment analysis

We start by searching the STRING website (http://string-db.org/) for the name of a single protein ("NF-κB1") and the name of an organism ("Homo sapiens"). Then, we set the following main parameters: minimum interaction score ["Low confidence (0.150)"], network edge meaning ("evidence"), maximum number of interactive users to display ("not more than 50 interactive users" in the first shell), and active each other sources ("experiments"). Last, the useable NF-κB1 conjugated proteins were gained.

We used the "similar gene detection" module of GEPIA2 to obtain the first 100 targeted genes related to NF-κB1 based on all normal tissue and TCGA tumor data sets. We also applied GEPIA2's "correlation analysis" module to NF- κB1 was paired with the selected gene for Pearson correlation analysis. Log2 TPM is used for point graphs. *P*-values and correlation coefficients (R) are given. In addition, the "gene_corr" module of TIMER2 was used to provide the heat map data of the selected genes, including partial correlation (COR) and purity adjusted p value of Spearman rank correlation test. We used the JVENN interactive Venn diagram viewer (19) for cross analysis to compare the NF-κB1 binding and interacting genes. In addition, we combined the two sets of data for KEGG (Kyoto Encyclopedia of Genes and Genomes) pathway analysis. In short, we uploaded the list of genes to DAVID (a database for annotation, visualization, and integrated discovery), set the selected identifiers ("OFFICIAL_GENE_SYMBOL") and species ("Homo sapiens"), and obtained the data for the functional annotated map. Finally, the enrichment path was visualized through "tidyr" and "ggplot2" R packets. In addition, the R package of "clusterProfiler" was used for GO (Gene Ontology) enrichment analysis. BP (Biological Process), CC (Cellular Component) and MF (Molecular Function) were visualized as Cnetplot. Use the CNETPLOT function (Circular = F, ColorEdge =T, NODE_LABEL =T) (20). SangerBox (http://sangerbox.com/Tool/) was used for this analysisDouble-tailed $P<0.05$ was considered statistically significant.

3 Results

3.1 Gene expression analysis data

In this study, we aimed to investigate the carcinogenic effect of NF-κB1 (NM_001165412 for mRNA, NP_001158884.1 Fig. S1a) in human. As shown in Fig S1b, the structure of NF-κB1 protein is conserved between different species (such as H. sapiens, P. troglodytes, M. mulatta, etc.), and is usually composed of Death_ NF-κB1_p105 (cd08797) domain, RHD-n (c108275) domain, DD (cl14633) and Ank_2

(pfam12796) domain, etc. Phylogenetic tree data (Fig. S2) showed the evolutionary relationships of NF-κB1 proteins among different species.

We first analyzed the expression profile of NF-κB1 in nontumor tissues and different cells. As shown in Fig. S3a, combined with HPA (Human protein atlas), GTEx and Fantom5 (Function annotation of the Mammalian genome 5) data set, the expression of NF-κB1 is the highest in lymph nodes, followed by bone marrow, appendix and thymus (Fig. S3a). However, NF-κB1 was expressed in all the tested tissues (all of which were consistent with the normalized expression value >1), showing a low RNA tissue specificity. When NF-κB1 expression was analyzed in different blood cells, low RNA blood cell type specificity also appeared in the HPA/Monaco/Schmiedel dataset (Fig. S3b).

We analyzed the expression status of NF-κB1 in different types of TCGA cancer using the TIMER2 method. As shown in Fig. 1a, NF-κB1 plays an important role in BLCA (Bladder Urothelial Carcinoma), BRCA (Breast invasive carcinoma), CHOL (Cholangiocarcinoma), COAD (Colon adenocarcinoma), HNSC (Head and Neck squamous cell carcinoma), HNSC-HPV (Head and Neck squamous cell carcinoma-human papillomavirus), LUSC (Lung squamous cell carcinoma), SKCM (Skin Cutaneous Melanoma), STAD (Stomach adenocarcinoma), THCA (Thyroid carcinoma), UCEC (Uterine Corpus Endometrial Carcinoma) (P<0.001), ESCA (Esophageal carcinoma) (P<0.01), GBM (Glioblastoma multiforme), KIRC (Kidney renal clear cell carcinoma), LUAD (Lung adenocarcinoma), PCPG (Pheochromocytoma and Paraganglioma), PRAD (Prostate adenocarcinoma), READ (Rectum adenocarcinoma), PAAD (Pancreatic adenocarcinoma), (P<0.05), were higher than those of the corresponding control tissues.

After using normal tissues from the GTEx dataset as controls, we further evaluated differences in NF-κB1expression between CHOL (Cholangiocarcinoma), DLBC (Lymphoid Neoplasm Diffuse Large B-cell Lymphoma), GBM (Glioblastoma multiforme), LAML (Glioblastoma multiforme), PAAD (Pancreatic adenocarcinoma), THYM (Thymoma) (Fig. 1b, P<0.05). However, for other tumors, we did not get significant differences, such as BLCA (Bladder Urothelial Carcinoma), COAD (Colon adenocarcinoma), ESCA (Esophageal carcinoma), LIHC (Liver hepatocellular carcinoma), KICH (Kidney Chromophobe), PCPG (Pheochromocytoma and Paraganglioma), as shown in Fig. S4a.

Results from the CPTAC dataset showed that total NF-κB1 protein was highly expressed in primary tissues of breast cancer, UCEC (Uterine Corpus Endometrial Carcinoma), ovarian cancer, LUAD (Lung adenocarcinoma) colon cancer, colon cancer, clear cell RCC, and LUAD (Lung adenocarcinoma) colon cancer (Fig. 1c, P<0.001) compared with normal tissues.

We also used the GEPIA2 “Pathological Stage Plot” module to observe the correlation between NF-κB1 expression and tumor pathological stage, including BRCA (Breast invasive carcinoma), KIRC (Kidney renal clear cell carcinoma) (Fig. 1d, P<0.05).

3.2 Survival analysis data

We divided tumor cases into high expression group and low expression group according to the expression level of NF-κB1, and mainly studied the correlation between NF-κB1 expression and prognosis of patients

with different tumors using TCGA and GEO data sets. As shown in Fig. 2a, high expression of NF-κB1 in TCGA was associated with poor overall OS (Survival) outcomes for CESC (*P*=0.02), LGG (*P*=0.019), LUSC (*P*=0.033), OV (*P*=0.026). Data from DFS (disease-free survival) analysis (Fig. 2b) showed that high NF-κB1 expression was not associated with poor prognosis for all types of tumors. In addition, low NF-κB1 gene expression was associated with poor OS prognosis for ACC(*P*=0.037), KIRC(*P*=0.00004), READ (*P*=0.035) (Fig. 2a, P=0.012) and DFS prognosis for KIRC (*P*=0.0014) (Fig. 2b, P=0.014).

Moreover, using Kaplan Meier mapping tool to analyze survival data, it was found that low expression of NF-κB1 was correlated with breast cancer OS (overall survival) (Fig. S7a, *P*=0.0000092), DMFS (survival without distant metastasis) (*P*=0.000035) and RFS (relapse-free survival) (*P*<0.001) prognosis. However, in ER status-IHC (positive and negative), ER status-arry (positive and negative), HER2 status (positive and negative), Grade2, Intrinsic subtype (Basal, LuminalA, LuminalB) and Pietenpol subtype (basal-like1, Luminal androgen receptor) breast cancer cases, high expression of NF-κB1 was associated with poor OS, RFS (relapsion-free survival) and DMFS prognosis (Table S1, *P*<0.05). Additionally, a low NF-κB1 expression level was associated with PFS (Progression Free Survival) (*P*=0.0005), prognosis for ovarian cancer (Fig. S5b). In contrast, high expression levels of NF-κB1was related to poor OS (*P*=0.019) and PPS (Post-progression survival) (*P*=0.0019) prognosis for lung cancer (Fig. S5c), FP (*P*=0.00083) prognosis for gastric cancer (Fig. S5d) and PFS (*P*=0.01) and RFS (*P*=0.0046) and DSS (*P*=0.035) prognosis for liver cancer. We also used the selected clinical factors to carry out a subgroup analysis and observed different conclusions. (Tables S1-S5). The above data suggested that the expression of NF-κB1 was different from the prognosis of patients with different tumors.

3.3 Genetic alteration analysis data

We observed genetic alterations in NF-κB1 in different tumor samples from the TCGA cohort. As shown in Figure 3a, the “mutant” uterine tumor patients had the highest frequency of NF-κB1 change (>6%). The “amplified” type of CNA was the dominant type of Pheochromocytoma and Paraganglioma, with a frequency of change of about 1% (Fig. 3a). Figure 3b further shows the types, loci and number of cases of NF-κB1 gene alteration. We found that missense mutations in NF-κB1 were the main type of genetic alterations. A520T/V alterations in the ANK_2 domain were detected in 1 UCEC cases, 1BRCA cases and 1 COAD cases (Fig. 3b), which can induce frame shift mutations in NF-κB1 gene, translating 520 NF-κB1 proteins from A (Alanine) to T/V (Threonine/valine), and subsequent NF-κB1 protein truncation. We can observe the A520T/V site in the 3D structure of NF-κB1 protein (Fig. 3c). In addition, we also explored the potential association between c gene alterations and clinical survival outcomes in patients with different types of cancer. The data in Fig. 3d shows that the prognosis of CUEC cases with NF-κB1 alteration is better in terms of disease-specific survival rate (*P* = 0.0811) and disease-free survival rate (*P* =0.096) than that of cases without NF-κB1 alteration. Additionally, we analyzed the association between NF-κB1 expression and TMB (tumor mutation burden)/MSI (microsatellite instability) in all TCGA tumor. As shown in Fig. S6, we observed that NF-κB1 expression of LUAD, BLCA, LIHC, BRCA, THCA and UVM was negatively correlated with TMB, while UCEC, COAD, STAD and LGG were positively correlated. The expression of NF-κB1 was also negatively correlated with PAD, BRCA, SKCM, HNSC, and DLBC (*P*<0.05),

and positively correlated with COAD, KIRC, and LAML (P<0.05) (Fig. S7). This result deserves further investigation.

3.4 DNA methylation analysis data

In the TCGA project, we used the MEXPRESS method to study the potential relationship between NF-κB1 DNA methylation and different tumor pathogenesis. For TGCT cases, we observed a significant negative correlation between DNA methylation and gene expression in NF-κB1 non promoter region, such as cg06501333 (P<0.001, R=0.527), as shown in Figure S8.

3.5 Protein phosphorylation analysis data

We also compared the phosphorylation levels of NF-κB1 in normal tissues and primary tumor tissues. CPTAC data sets were used to analyze five types of tumors (breast cancer, ovarian cancer, LUAD, UCEC and clear cell RCC,). Fig. 4a summarizes the NF-κB1 phosphorylation sites and their significant differences. Compared with normal tissues, S893 within the NF-κB1 DEATH domain showed higher phosphorylation levels in all primary tumor tissues (Fig. 4a-g, all P <0.05), the next is the increase of phosphorylation level of S892 locus in the breast cancer death area. (Fig. 4b, P=0.00000049), clear cell RCC (Fig. 4c, P=0.1), LUAD (Fig. 4d, P=0.033). We also analyzed NF-κB1 phosphorylation identified by CPTAC using the PhosphoNET database, and found that the NF-κB1 phosphorylation of S893 in cell cycle was supported by a published article (21).

3.6 Immune infiltration analysis data

As an important part of tumor microenvironment, tumor infiltrating immune cells are closely related to tumor occurrence, progression or metastasis (22, 23). Tumor associated degmacyte in tumor microenvironment have been reported to be involved in adjusting the function of various tumor soaking immunocyte (24, 25). Here, we used TIMER, CIBERSORT, CIBERSORT-ABS, QUANTISEQ, XCELL, MCPCOUNTER and EPIC algorithms to investigate the potential relationship between different levels of immune cell infiltration and NF-κB1 gene expression in different types of TCGA tumors. Through a series of analyses, we find that the immune infiltration of $CD8^+$ T cells is negatively correlated with the expression of NF-κB1 in THYM (Thymoma) (Fig.S9a-b). In addition, we observed that the expression of NF-κB1 was positively correlated with the invasion value of cancer-associated fibroblasts in TCGA tumors of LGG, LIHC, LUSC, RAAD and TGCT (Fig. 5). The above tumor scatter plot data obtained by an algorithm are shown in Fig. 5 and Fig. S9. For instance, because of the MCPCOUNTER algorithm, expression levels NF-κB1 in TGCT is positively correlated with the infiltration level of cancer-associated fibroblasts (Fig. 5, Rho= -0.621, P=5.12E-17)

3.7 Enrichment analysis of NF-κB1-related partners

In order to better understand the molecular mechanism of NF-κB1 gene in tumorigenesis. Through a series of pathway enrichment analysis, we tried to screen the target proteins bound to NF-κB1 and the

related genes expressed by NF-κB1. We used the string tool to obtain a total of 50 NF- κB1 binding protein was sustained by experimental evidence. The interaction network between these proteins is shown in Figure 6a. Using GEPIA2 tool in combination with all tumor expression data of TCGA, we obtained the first 100 genes expressed by NF- κB1. In Fig. 6b, the expression level of NF- κB1 was positively correlated with UBE2D3 (R=0.63), IRF2 (R=0.63), ELF1 (R=0.58), ERAP1 (R=0.56), SMNDC1 (R=0.56) genes (all P<0.001). The corresponding heat map data also demonstrated that NF-κB1 was positively correlated with the above 5 genes in most explicit cancer types (Fig. 6c). By cross analysis, the two groups had 6 members, namely UBE2D3, SP1, STAT3, TNFAIP3, CNOT6L, RIPK1 (Fig. 6d).

We combined these two data sets for KEGG and GO enrichment analysis. The KEGG data in Figure 6e suggest that “endoplasmic reticulum protein processing” and “metabolic pathway” may be participated in NF-κB1 effect on tumor etiopathogenesis.

4 Discussion

NF-κB1 has been reported in almost all animal cell types and is an important regulator of autoimmune diseases, cell proliferation, apoptosis and stress response (26). In this study, our “HomoloGene” and phylogenetic tree analysis data also showed that NF-κB1 protein structure was conserved among different species, indicating that there may be a similar mechanism for the normal physiological function of NF-κB1. Newly published publications report a functional association between NF-κB1 and clinical diseases, especially tumors (11–13, 27–29). It is not clear whether NF-κB1 plays a role in the pathogenesis of different tumors through some common molecular mechanisms. Through the search of network literature, we were unable to retrieve any publications that performed pan-cancer analysis of NF-κB1 from the perspective of the whole tumor. Therefore, based on TCGA, CPTAC and GEO database data, we combined the molecular characteristics of gene expression, gene alteration, DNA methylation or protein phosphorylation to comprehensively detect NF-κB1 gene in 33 different tumors.

NF-κB1 is highly expressed in most tumors. However, NF-κB1 gene survival analysis data have yielded different conclusions for different tumors. For liver cancer, we performed a set of survival analyses using the Kaplan Meier mapping method (30), including liver cancer cases in the GSE20017/GSE9843 cohort. The high expression of NF-κB1 is related to the clinical prognosis of overall survival, progression free survival, relapse free survival and Disease specific survival. However, the role of NF-κB1 expression on clinical prognosis of hepatocellular carcinoma needs more clinical big data to confirm.

With regard to lung cancer, we analyzed the data sets of TCGA-LUSC (n=483) and TCGA-LUAD (n=483) projects and found that NF-κB1 over-expression was associated with poor overall survival and prognosis in lung squamous cell carcinoma (P=0.033), but not in lung adenocarcinoma (Fig. 2a). However, after analyzing 1926 lung cancer cases of CAARRAY, GSE14814, GSE19188, and GSE29013, NF-κB1 over-expression was associated with overall survival, first progression, and post-progression survival prognosis, especially in lung adenocarcinoma cases (Table S2). Consequently, a larger sample capacity

is demanded to confirm the role of NF-κB1 in the subsist and prognosis of patients with different types of carcinoma of the lungs.

In ovarian cancer, based on GEO data (GSE14764, GSE15622, GSE18520, GSE19829, etc.), we have observed that low NF-κB1 expression was associated with adverse clinical outcomes in progression-free survival of ovarian cancer, especially in “stage3/4”, “grade 3”, “TP53 mutation Mutated” and “Debulk” (Table S3). Similarly, it has been reported that NF-κB1 can advance the invasion and remove of cervical cancer cells (31). Our survival analysis based on TCGA shows that the low expression of NF-κB1 is associated with adverse clinical prognosis of cervical cancer. Since the TCGA-TCGT cohort only contains tumor data, we used normal testicular tissues from GTEx data set as controls and found that the level of NF-κB1 in TGCT tissues was higher than that in normal tissues. However, NF-κB1 overexpression seems to be associated with good clinical outcomes in patients with TGCT.

Some studies have reported the role of high expression of NF-κB1 in regulating the occurrence of breast cancer (11, 12, 32, 33). Surprisingly, survival data of Kaplan-Meier plotters based on Affymetrix HGU133A and HGU133+2 microarrays (34). we discover that the low expression of NF-κB1 was interrelated with poor overall survival, distance metastasis free survival and recurrence free survival of mammary gland cancer patients.

In this study, we present for the first time evidence of a potential association between NF-κB1 expression and TMB or MSI in all TCGA tumors. In addition, we integrated information on NF-κB1 combine ingredients and NF-κB1 expression related genes in all tumors. Then a series of enrichment analyses were carried out to determine the potential effects of "metabolic pathway", "endoplasmic reticulum protein processing" and RNA metabolism in tumor etiology or pathogenesis. Through a variety of immune deconvolution methods, we observed that there was a statistically negative correlation between the level of $CD8^+$ T cell infiltration and the expression of NF-κB1 in thymic tumors. Our results suggest for the first time that the expression of NF-κB1 is relevant to the level of tumor infiltrating fibroblasts in some tumors. In order to explain the difference of NF-κB1 overexpression in the above-mentioned tumors, in contrast, this high expression status is related to the favorable prognosis of the patients. First of all, it is noteworthy that the NF-κB1 high expression group and NF-κB1 low expression group, including TGCT and UCEC, did not exceed 100 cases. A larger sample may be needed to testify the above-mentioned conclusion. Second, further molecular experimental evidence is needed to judge whether the high expression of NF-κB1 plays an important role in the occurrence of these tumors, or whether it is only the result of tumor drug resistance in normal tissues.

In TGCT patients of TCGA, we observed a potential correlation between the decrease of DNA methylation status and the high expression of NF-κB1 in the non-promoter region. Different methylation sites also have NF-κB1 methylation differences in TGCT tissue matching normal tissue. More evidence is needed for the potential role of DNA methylation of NF-κB1 in the pathogenesis of TGCT.

We first studied the molecular mechanism of NF-κB1 protein in breast cancer, lung adenocarcinoma, endometrial carcinoma, ovarian cancer and clear cell renal cell carcinoma from the perspective of total protein and phosphoprotein by CPTAC data set. The results of this study showed that compared with normal controls, the expression level of total NF-κB1 protein was higher in primary tumors, and the phosphorylation level of S893 in the DEATH domain was higher. However, we still cannot rule out that the high-level phosphorylation of S893 NF-κB1 is a by-product indicated by tumor cells and has no functional meaning in tumor cells. The role of NF-κB1 phosphorylation at S893 site and its related cell cycle regulation in tumorigenesis needs to be further studied.

In conclusion, our first pan cancer analysis of NF-κB1 showed that NF-κB1 expression was significantly correlated with clinical prognosis, DNA methylation, protein phosphorylation, immune cell infiltration, tumor mutation burden or microsatellite instability in a variety of tumors. This helps to understand the role of NF-κB1 in tumorigenesis from the perspective of clinical tumor samples.

Declarations

Data Availability

The datasets generated/analyzed during the current study are available.

Acknowledgements

These studies were supported by the Natural Science Foundation of Guangxi (No. 2018GXNSFBA050045) and Science and Technology Base and Special Talent of Guangxi (No. AD19110016).

Author Contributions

Lihong Huang: Conceptualization, Methodology, Validation, Investigation, Writing - Original Draft, Visualization

Ruoling Zheng: Formal analysis, Investigation, Resources, Data Curation

Hua-song Gong*: Supervision, Project administration

Yong-chao Qiao*: Writing - Review & Editing, Funding acquisition

All authors contributed to the article and approved the submitted version.

Funding

This work was supported by the Natural Science Foundation of Guangxi (No. 2018GXNSFBA050045) and Science and Technology Base and Special Talent of Guangxi (No. AD19110016).

Ethical Approval

This study did not involve human or animal experiments and no ethical certification was required.

Competing Interests

The authors reported no declarations of interest.

References

1. Hutter C, Zenklusen JC. 10.1016/j.cell.2018.03.042. The Cancer Genome Atlas: Creating Lasting Value beyond Its Data. Cell. 2018;173(2):283–285.
2. Zhang Z, Li H, Jiang S, Li R, Li W, Chen H, et al. 10.1093/bib/bby023. A survey and evaluation of Web-based tools/databases for variant analysis of TCGA data. Brief Bioinform. 2019;20(4):1524–1541.
3. Clough E, Barrett T. 10.1007/978-1-4939-3578-9_5. The Gene Expression Omnibus Database. Methods Mol Biol. 2016;1418:93–110.
4. Concetti J, Wilson CL. 10.3390/cells7090133. NFKB1 and Cancer: Friend or Foe? Cells. 2018;7(9).
5. Chatzikyriakidou A, Kyriakou A, Meltzanidou P, Lambropoulos A, Patsatsi A. 10.1111/exd.13957. Association of NFKB1 -94ATTG ins/del polymorphism (rs28362491) with pemphigus vulgaris. Exp Dermatol. 2019;28(8):972–975.
6. Wang M, Wang Z, Zhu X, Guan S, Liu Z. 10.1007/s11626-019-00370-3. NFKB1-miR-612-FAIM2 pathway regulates tumorigenesis in neurofibromatosis type 1. In Vitro Cell Dev Biol Anim. 2019;55(7):491–500.
7. Zhou F, Zhu Z, Gao J, Yang C, Wen L, Liu L, et al. 10.1016/j.cellimm.2018.04.016. NFKB1 mediates Th1/Th17 activation in the pathogenesis of psoriasis. Cell Immunol. 2018;331:16–21.
8. Tan X, Zhang X, Pan L, Tian X, Dong P. 10.1155/2017/4323496. Identification of Key Pathways and Genes in Advanced Coronary Atherosclerosis Using Bioinformatics Analysis. Biomed Res Int. 2017;2017:4323496.
9. Nguyen DP, Li J, Yadav SS, Tewari AK. 10.1111/bju.12488. Recent insights into NF-κB signalling pathways and the link between inflammation and prostate cancer. BJU Int. 2014;114(2):168–176.
10. Gao J, Xu HL, Gao S, Zhang W, Tan YT, Rothman N, et al. 10.1136/bmjopen-2013-004427. Genetic polymorphism of NFKB1 and NFKBIA genes and liver cancer risk: a nested case-control study in Shanghai, China. BMJ Open. 2014;4(2):e004427.
11. Kuo WY, Hwu L, Wu CY, Lee JS, Chang CW, Liu RS. 10.7150/thno.16827. STAT3/NF-κB-Regulated Lentiviral TK/GCV Suicide Gene Therapy for Cisplatin-Resistant Triple-Negative Breast Cancer. Theranostics. 2017;7(3):647–663.
12. Kancharla J, Prasad IDV, Bhaskar L, Bramhachari PV, Alam A. 10.2174/1389200221666200310113118. Meta-analysis of NFKB1-94 ATTG Ins/Del Polymorphism and Risk of Breast Cancer. Curr Drug Metab. 2020;21(3):221–225.

13. Chen LP, Cai PS, Liang HB. 10.4238/2015.July.27.15. Association of the genetic polymorphisms of NFKB1 with susceptibility to ovarian cancer. Genet Mol Res. 2015;14(3):8273–8282.
14. Tang Z, Li C, Kang B, Gao G, Li C, Zhang Z. 10.1093/nar/gkx247. GEPIA: a web server for cancer and normal gene expression profiling and interactive analyses. Nucleic Acids Res. 2017;45(W1):W98-w102.
15. Zhou Y, Lih TM, Pan J, Höti N, Dong M, Cao L, et al. 10.1186/s13045-020-01013-x. Proteomic signatures of 16 major types of human cancer reveal universal and cancer-type-specific proteins for the identification of potential therapeutic targets. J Hematol Oncol. 2020;13(1):170.
16. Tang Z, Kang B, Li C, Chen T, Zhang Z. 10.1093/nar/gkz430. GEPIA2: an enhanced web server for large-scale expression profiling and interactive analysis. Nucleic Acids Res. 2019;47(W1):W556-w560.
17. Katsuta E, Rashid OM, Takabe K. 10.3390/ijms21113890. Fibroblasts as a Biological Marker for Curative Resection in Pancreatic Ductal Adenocarcinoma. Int J Mol Sci. 2020;21(11).
18. Bangi E. 10.3390/ijms21113754. Strategies for Functional Interrogation of Big Cancer Data Using Drosophila Cancer Models. Int J Mol Sci. 2020;21(11).
19. Nagpal S, Kuntal BK, Mande SS. 10.1093/bioinformatics/btaa723. NetSets.js: a JavaScript framework for compositional assessment and comparison of biological networks through Venn-integrated network diagrams. Bioinformatics. 2021;37(4):580–582.
20. Yu G, Wang LG, Han Y, He QY. 10.1089/omi.2011.0118. clusterProfiler: an R package for comparing biological themes among gene clusters. Omics. 2012;16(5):284–287.
21. Fujimoto K, Yasuda H, Sato Y, Yamamoto K. 10.1016/0378-1119(95)00507-3. A role for phosphorylation in the proteolytic processing of the human NF-kappa B1 precursor. Gene. 1995;165(2):183–189.
22. Dieu-Nosjean MC, Giraldo NA, Kaplon H, Germain C, Fridman WH, Sautès-Fridman C. 10.1111/imr.12405. Tertiary lymphoid structures, drivers of the anti-tumor responses in human cancers. Immunol Rev. 2016;271(1):260–275.
23. Lopes M, Gonzaga AKG, Mosconi C, Palomino GM, Mendonça EF, Batista AC, et al. 10.1016/j.archoralbio.2018.09.017. Immune response and evasion mechanisms in lip carcinogenesis: An immunohistochemical study. Arch Oral Biol. 2019;98:99–107.
24. Dzobo K, Dandara C. 10.1089/omi.2020.0023. Architecture of Cancer-Associated Fibroblasts in Tumor Microenvironment: Mapping Their Origins, Heterogeneity, and Role in Cancer Therapy Resistance. Omics. 2020;24(6):314–339.
25. Yoshida GJ. 10.1186/s13046-020-01611-0. Regulation of heterogeneous cancer-associated fibroblasts: the molecular pathology of activated signaling pathways. J Exp Clin Cancer Res. 2020;39(1):112.
26. Cartwright T, Perkins ND, C LW. 10.1111/febs.13627. NFKB1: a suppressor of inflammation, ageing and cancer. Febs j. 2016;283(10):1812–1822.

27. Li L, Zhang ZT. 10.1155/2019/6523837. Genetic Association between NFKBIA and NFKB1 Gene Polymorphisms and the Susceptibility to Head and Neck Cancer: A Meta-Analysis. Dis Markers. 2019;2019:6523837.
28. Li D, Wu C, Cai Y, Liu B. 10.1177/1010428317717107. Association of NFKB1 and NFKBIA gene polymorphisms with susceptibility of gastric cancer. Tumour Biol. 2017;39(7):1010428317717107.
29. Yang D, Zhang W, Liang J, Ma K, Chen P, Lu D, et al. 10.18632/oncotarget.23587. Single cell whole genome sequencing reveals that NFKB1 mutation affects radiotherapy sensitivity in cervical cancer. Oncotarget. 2018;9(7):7332–7340.
30. Menyhárt O, Nagy Á, Győrffy B. 10.1098/rsos.181006. Determining consistent prognostic biomarkers of overall survival and vascular invasion in hepatocellular carcinoma. R Soc Open Sci. 2018;5(12):181006.
31. Pallavi S, Anoop K, Showket H, Alo N, Mausumi B. 10.1007/s13277-015-3312-7. NFKB1/NFKBIa polymorphisms are associated with the progression of cervical carcinoma in HPV-infected postmenopausal women from rural area. Tumour Biol. 2015;36(8):6265–6276.
32. Kim GC, Kwon HK, Lee CG, Verma R, Rudra D, Kim T, et al. 10.1038/s41389-018-0101-3. Upregulation of Ets1 expression by NFATc2 and NFKB1/RELA promotes breast cancer cell invasiveness. Oncogenesis. 2018;7(11):91.
33. Betancur PA, Abraham BJ, Yiu YY, Willingham SB, Khameneh F, Zarnegar M, et al. 10.1038/ncomms14802. A CD47-associated super-enhancer links pro-inflammatory signalling to CD47 upregulation in breast cancer. Nat Commun. 2017;8:14802.
34. Györffy B, Lanczky A, Eklund AC, Denkert C, Budczies J, Li Q, et al. 10.1007/s10549-009-0674-9. An online survival analysis tool to rapidly assess the effect of 22,277 genes on breast cancer prognosis using microarray data of 1,809 patients. Breast Cancer Res Treat. 2010;123(3):725–731.

Figures

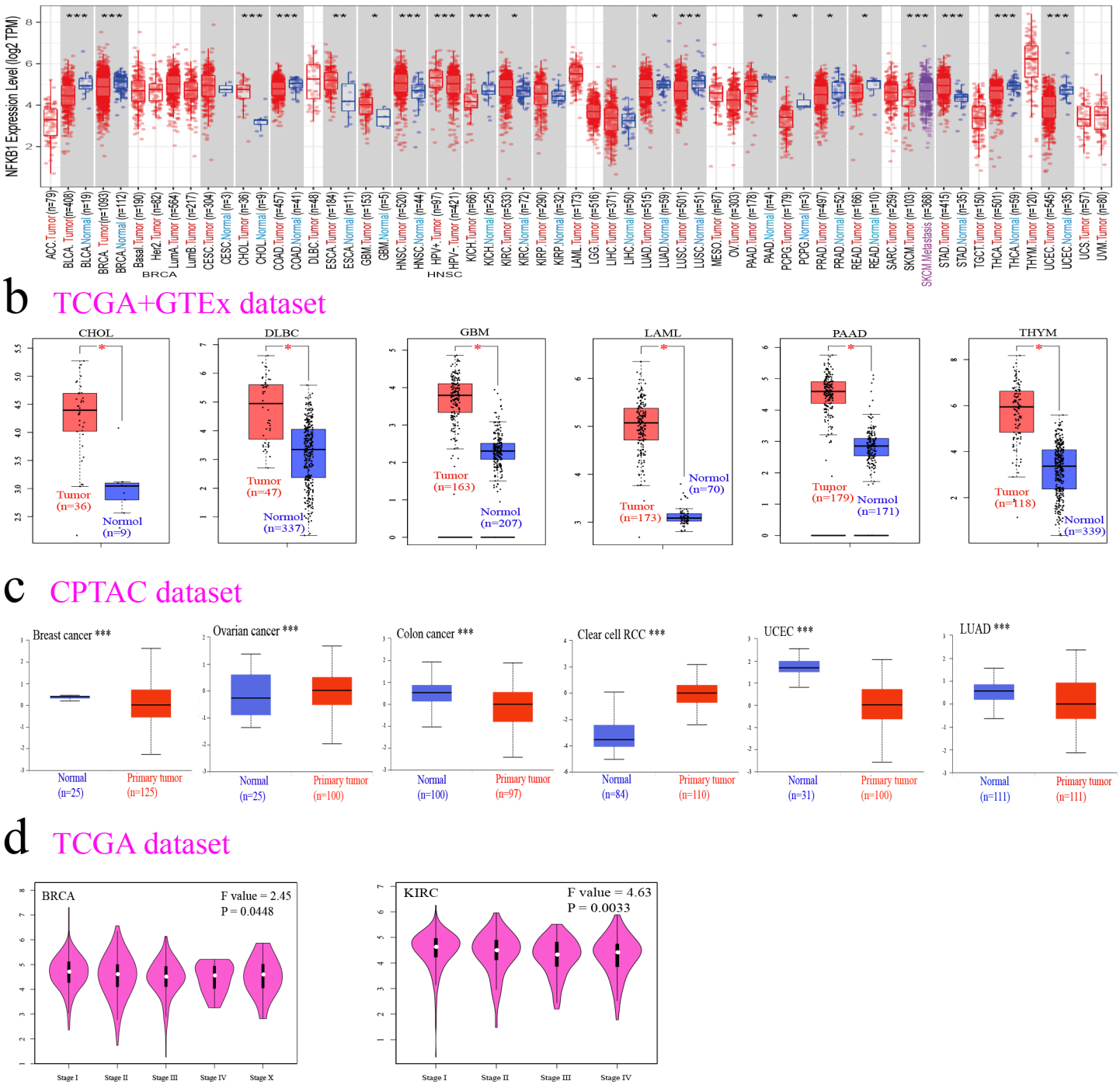

Figure 1

Expression level of NF-κB1 gene in different tumors and pathological stages. (a) The expression of NF-κB1 gene in specific cancer subtypes or different cancers was analyzed through TIMER2. * P<0.05; ** P<0.01; *** P<0.001. (b) For the type of CHOL, DLBC, GBM, LAML, PAAD, THYM and THYM in the TCGA project, the corresponding normal tissues in the GTEx database were used as controls. Provide box chart data. ** P <0.01. (c) Based on the CPTAC dataset, we also analyzed the expression level of NF-κB1 total protein between normal tissue and primary tissue of breast cancer, ovarian cancer, colon cancer, clear cell RCC and UCEC. *** P<0.001. (d) According to TCGA data, the expression level of NF-κB1 gene was

analyzed by the major pathological stages (I, II, III, IV) of BRCA and KIRC. Log2 (TPM+1) was used for logarithmic scale.

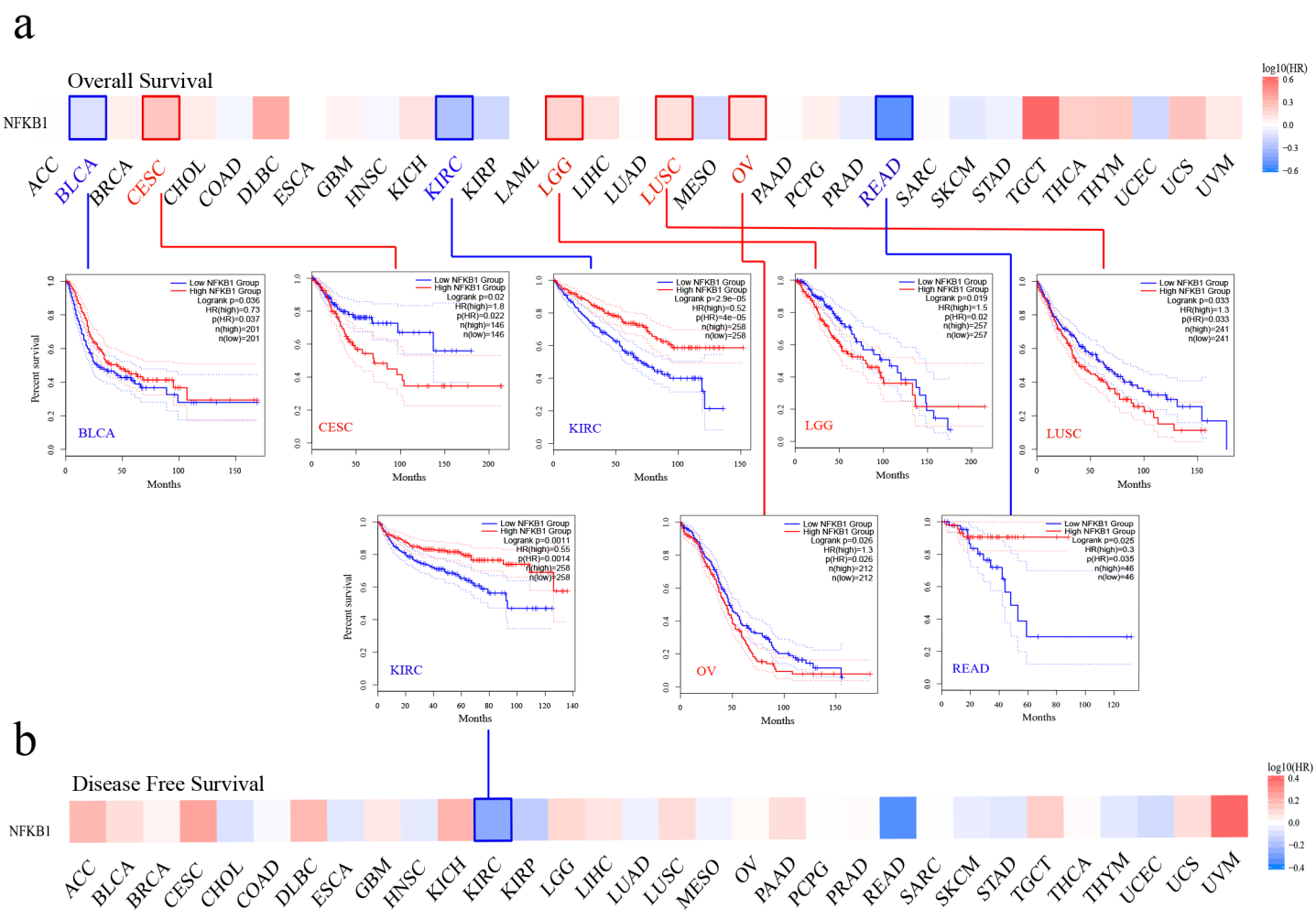

Figure 2

Relationship between NF-κB1 gene expression and tumor survival prognosis in TCGA. We used the GEPIA2 tool to analyze overall survival (a) and disease-free survival (b) of different tumors in TCGA by NF-κB1 gene expression. Survival graphs and Kaplan-Meier curves of positive results are given.

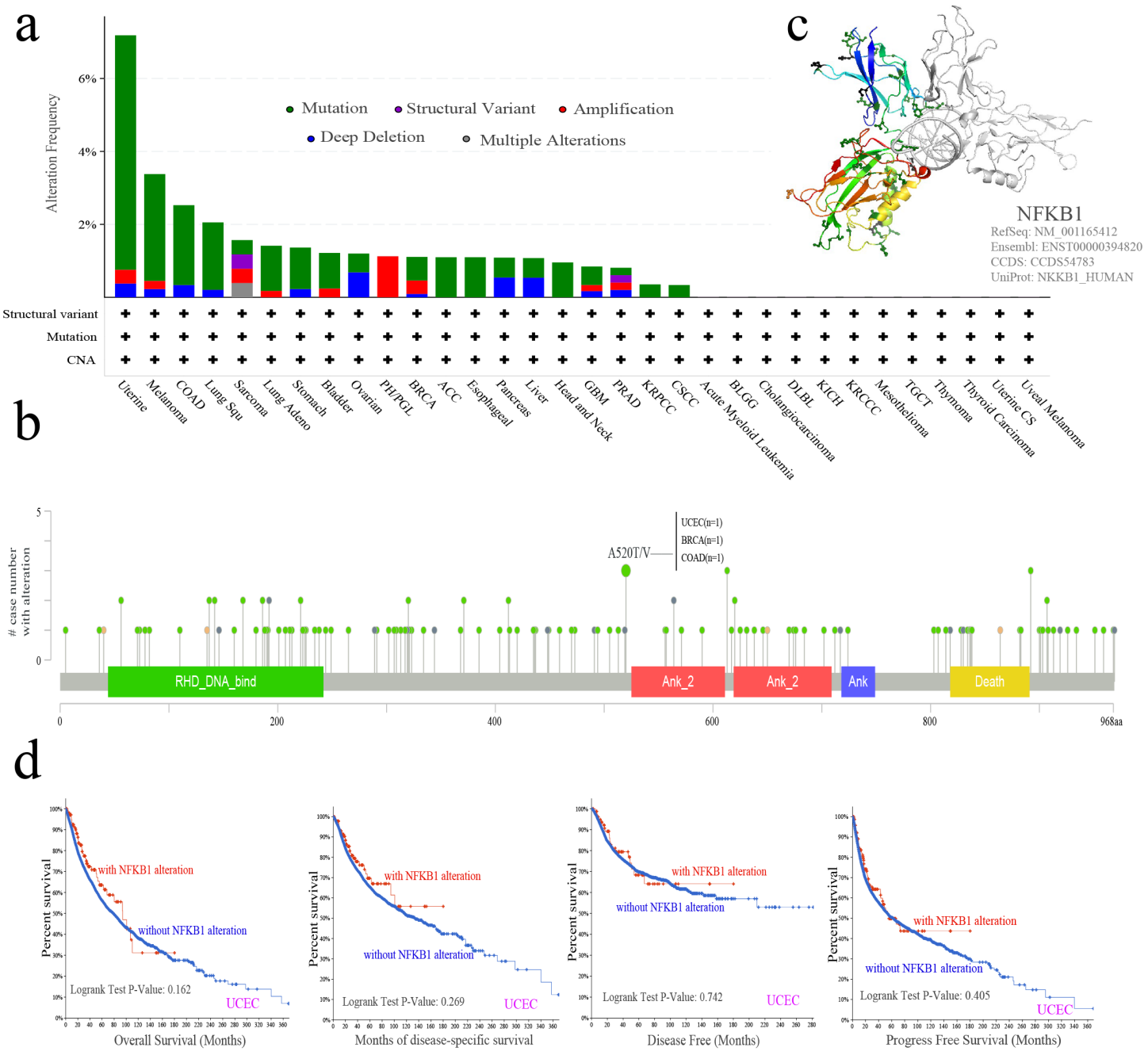

Figure 3

Mutation characteristics of NF-κB1 in different tumors of TCGA. We used the cBioPortal tool to analyze the mutation characteristics of NF-κB1 in TCGA tumors. Displays the frequency of mutation type (a) and mutation site (b). 3D structure of NF-κB1 (c). We also analyzed the potential association between mutat status and overall, disease-specific, disease-free and progression-free survival of UCEC (d) using the cBioPortal tool.

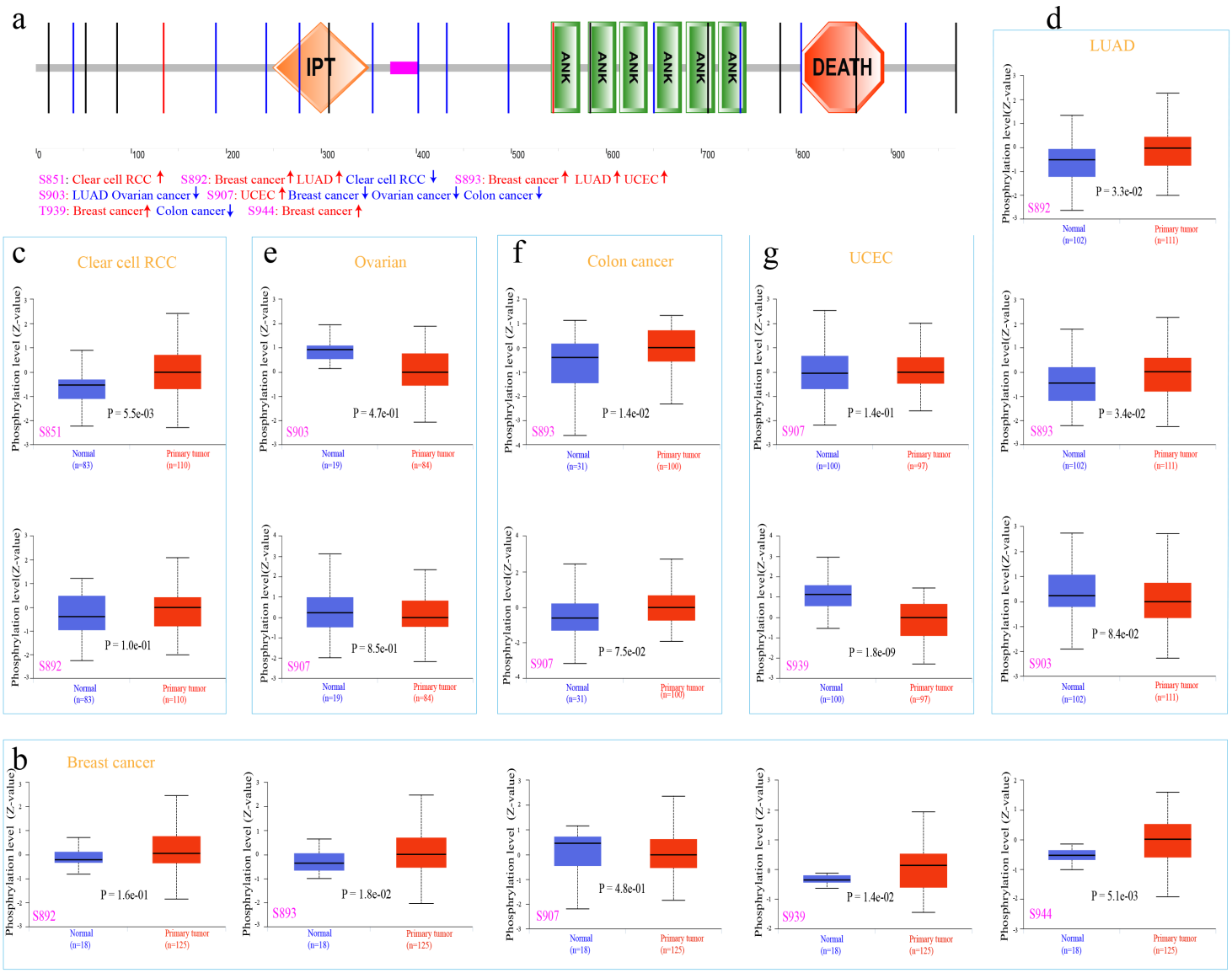

Figure 4

Phosphorylation analysis of NF-κB1 protein in different tumors. Based on the CPTAC dataset, the expression levels of NF-κB1 phosphorylated protein (NP_001158884.1,851, S892, S893, S903, S907, T939 and S944 sites) in normal tissue and primary tissue were analyzed by UALCAN. The phosphorylated protein sites with positive results are shown in NF-κB1 protein schematic map(a). We also provided the box maps for different cancers, including breast cancer (b), clear cell RCC (c), LUAD (d), ovarian cancer(e), UCEC (f), and colon cancer (g).

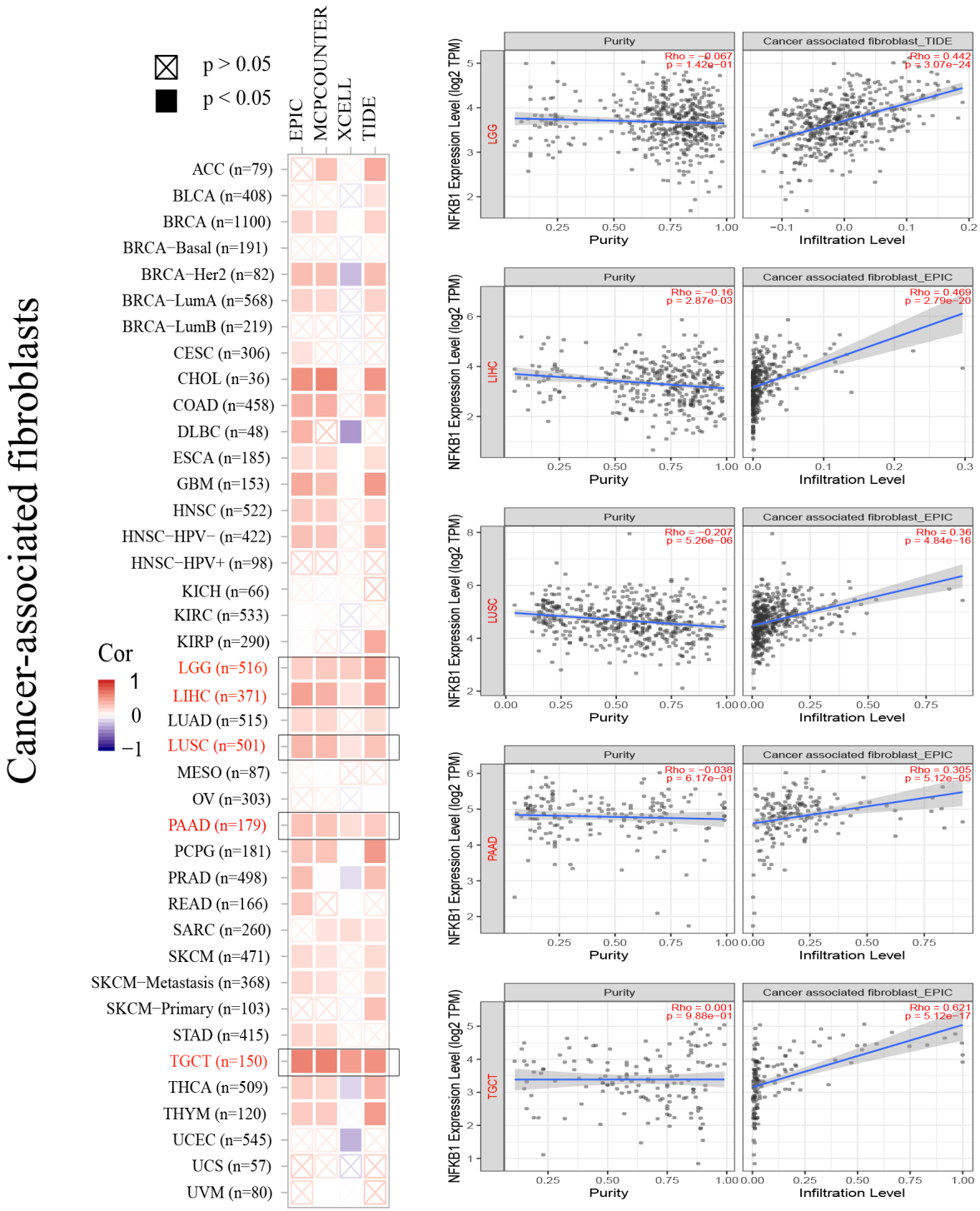

Figure 5

Correlation analysis of NF-κB1 expression and immune infiltration in cancer-associated fibroblasts. The potential correlation between the expression level of NF-κB1 gene in TCGA and the infiltration level of cancer-associated fibroblasts in all types of cancer was investigated using different algorithms.

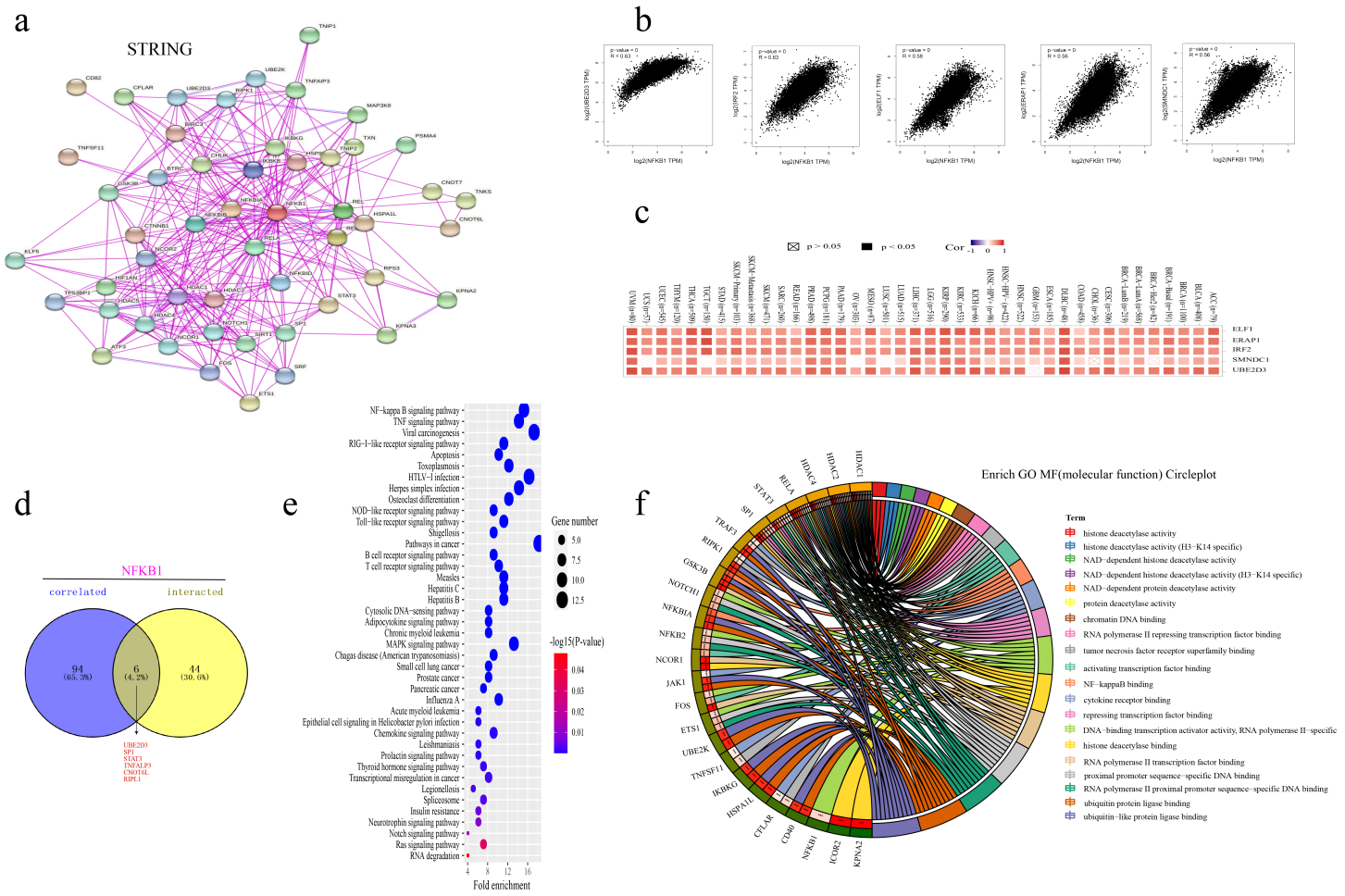

Figure 6

NF-κB1-related gene enrichment analysis. (a) We first obtained a usable experimentally determined NF-κB1 binding protein using the STRING tool. (b) The first 100 NF-κB1 related genes in TCGA project were obtained by GEPIA2 method, and the expression correlation of NF-κB1 with selected target genes TBL2, Plod3, CALU, GCC1 and MyBBP1A was analyzed. (c) Displays heat map data corresponding to detailed cancer types. (d) NF-κB1 binding and related genes were cross-analyzed. (e) KEGG pathway analysis was performed based on NF-κB1 binding and interacting genes. (f) The circle plot of the molecular function data in GO analysis.

Supplementary Files

This is a list of supplementary files associated with this preprint. Click to download.

- supplementarydocument.docx
- tablessupplementarydocument.docx
- S1.tif
- S20.85.tif

- S3.tif
- S4.tif
- S5.tif
- S6.tif
- S7.tif
- S8.tif
- S9.tif
- S10.tif